

Real-Time Detection Of Multiple Lesions During High Intensity Focused Ultrasound (HIFU) Treatments

Ralf Seip¹, Jahangir Tavakkoli¹, Adam Wunderlich¹, Narendra T. Sanghvi¹, Kris A. Dines², and Lawrence A. Crum³

¹Focus Surgery, Inc., Indianapolis, IN 46226, USA

²XDATA Corp., Indianapolis, IN 46220, USA

³APL, University of Washington, Seattle, WA 98105, USA

Abstract. This work describes the development of a non-invasive real-time technique to detect changes in tissue caused by the production of multiple lesions during a HIFU treatment sequence. It is based on estimation of relative changes in tissue properties derived from backscattered RF data, such as speed of sound, density, absorption coefficient, backscattering power, etc., as a function of HIFU exposure. The HIFU-induced changes were studied using a modified Sonablate[®] HIFU device. It makes use of a confocal 4 MHz pulse-echo ultrasound imaging transducer coupled with a HIFU delivery source on the same crystal. During the HIFU exposure period, every 0.5s the dosage delivery was interrupted for a short time (<80ms) and RF echo signals were acquired using the confocal imaging transducer. Using thermocouples, the temperatures at several locations in tissue were measured to correlate with the changes in tissue parameters. The RF data were digitized using a 50 MHz, 12-bit A/D converter and used for real-time as well as off-line processing and analysis. Several time- and frequency-domain echo RF processing algorithms were developed and tested through *in vitro* chicken breast and *in vivo* canine prostate experiments to estimate changes in tissue parameters in real time. Among these, the time-domain algorithms showed better correlation to gross pathology of HIFU-induced lesions in tissue. Work is in progress to implement the algorithm-of-choice in the Sonablate[®] device for clinical applications in human prostate cancer treatments.

INTRODUCTION

Lesion detection enables users to monitor HIFU treatments non-invasively and in real-time. It also enables them to obtain treatment feedback to determine whether the desired tissue location (e.g. a tumor) is being ablated sufficiently, and to make appropriate corrections if it is not (treatment control). Finally, lesion detection provides a quantitative tool to evaluate HIFU treatments after their completion.

All ultrasound lesion detection techniques are based on the hypothesis that the backscattered RF ultrasound signal acquired from the focal zone of the HIFU transducer during treatment contains information which can be extracted using signal processing techniques to monitor and image (either directly or indirectly) the HIFU-induced lesion. Previous work in this area demonstrates that the backscattered RF signal does indeed contain information that potentially can be used for lesion detection, treatment control, and evaluation [1, 2, 3, 4, 5, 6].

Most of this work has focused on detecting or imaging a single lesion. Clinically, however, the detection of multiple lesions is required, since all current clinical HIFU treatments treat large tissue volumes via the consecutive placement of multiple elementary lesions [7, 8, 9]. Extending single-lesion detection algorithms to multiple-lesion detection imposes new challenges: tissue properties change from one HIFU shot to the next, requiring adaptive or dynamic algorithms. The verification of the accuracy of such algorithms is also challenging, since individual lesions can merge to form a single contiguous lesion, some HIFU shots may not create the expected lesion, and ambiguities exist that are associated with detecting lesions created in locations where a lesion has already been created.

Imaging ultrasound-based lesion detection as a *visual* treatment feedback (based on B-mode images) is already being used with some success in clinical applications of the Sonablate[®] system for the non-invasive treatment of benign prostatic hyperplasia (BPH) and localized prostate cancer (PC) [8]. Not all HIFU-created lesions are seen in B-mode images, however. A different approach for multiple lesion detection and visualization is required. This paper describes the development of non-invasive techniques to detect the relative changes in tissue caused by the production of multiple HIFU lesions during a prostate treatment sequence for *automated* treatment feedback, control and evaluation (based on the analysis of RF backscattered data), and their real-time implementation and *in vivo* testing in the Sonablate[®] 500 HIFU system.

MATERIALS AND METHODS

To support the development of the multiple lesion detection algorithms, RF backscattered data was acquired with the imaging transducer of the Sonablate[®] 500 system, and stored for off-line processing. The imaging transducer (4MHz, 35% FBW Transmit/Receive Mode) is confocally aligned with the HIFU therapy transducer enabling accurate imaging of the HIFU-generated lesions in the prostate, as shown in Figure 1.

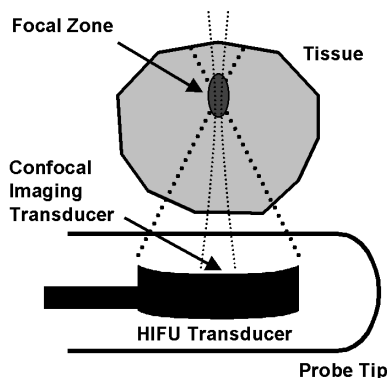


FIGURE 1. Confocal arrangement of the imaging transducer with the therapy transducer inside the transrectal probe tip enables accurate collection of RF ultrasound backscattered data lines (1D) which include the therapy transducer focal zone before, during, and after the HIFU lesion creation in the prostate.

RF backscattered data is sampled at 50 MHz (4096 points total, corresponding to an imaging depth of 61 mm), and always images a region containing the focal zone of the therapy transducer, located at 25, 30, 35, 40 or 45 mm for various focal-depth probes. 1D signals from the tissue containing the focal zone are collected before, during, and after the creation of each HIFU lesion for each HIFU lesion (300 to 600 elementary lesions are required to ablate an entire prostate for typical HIFU prostate cancer treatments). To acquire interference-free RF backscattered data during the HIFU "ON" time, HIFU delivery is briefly interrupted for <80 ms. 32 individual RF signals are acquired and averaged to generate a single RF echo signal every 500 ms. Reference data is acquired for each lesion site once at the beginning of the treatment before any HIFU energy has been delivered to the tissue (Pre-Treatment Reference Line, at $T=-\infty$), and then again before the particular site is treated (Pre-Lesion Reference Line, at $T=0s$). The data acquisition methodology followed for each lesion site is shown in Figure 2.

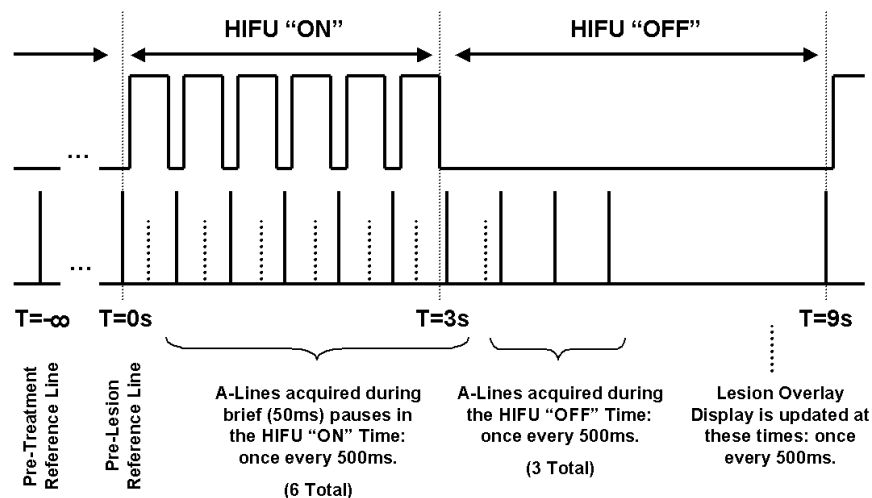


FIGURE 2. Acquisition methodology followed to acquire RF backscattered data for each lesion site before, during, and after the lesion creation. Note: the RF backscattered data contains pre-focal, focal, and post-focal imaging data. The top trace shows the brief HIFU interruptions that enable the acquisition of interference-free imaging data (1D), indicated by the vertical solid bars on the bottom trace.

Data was collected from *in vitro* turkey tissue to verify the data acquisition methodology and implementation in the Sonablate[®]500 HIFU system. Canine whole prostate HIFU ablation experiments (N=4) were performed to collect *in vivo* data. This data was processed both in real-time on the Sonablate[®]500 during the HIFU treatment to evaluate the lesion detection algorithm in a clinical setting, and stored for additional off-line analysis. During the *in vivo* evaluation, detection algorithm results were displayed as real-time color overlays on the B-mode images of the current treatment site acquired pre-treatment (see Figure 3), to indicate the estimated size and location of each lesion, both during and after the HIFU exposure. The dashed vertical bar in Figure 2 indicates when this lesion overlay update occurs. This allows the user to follow the actual lesion formation process.

LESION DETECTION ALGORITHMS

Several multiple-lesion detection algorithms have been examined as part of this research, and are briefly described below. New candidates are constantly being evaluated against the stored *in vivo* data for their ability to detect HIFU-induced multiple lesions and image tissue changes (either directly or indirectly), including wavelet approaches, adaptive filtering approaches (linear and/or non-linear), and template matching approaches. All algorithms use pre-lesion reference lines for calibration and/or normalization purposes.

In all approaches, $p(n, T)$ is the parameter indicative of the lesion displayed as a color overlay during the HIFU treatment, n is the index into the echo data (in depth, or "fast time"), and T is the index selecting the RF signal data lines (in treatment time, or "slow time"). $Echo(n, T_0)$ refers to the pre-lesion reference line, and $echo(n, T)$ refers to the RF backscattered data acquired at time T (every 500 ms) for the current lesion site. For analysis and display, $p(n, T)$ is computed for pre-focal, focal, and post-focal regions to localize the lesion in depth n , using windowed signal echo data (Blackman window, 1.5 to 3.5 mm long). $T - \Delta T$ references the previously acquired echo.

Signal Energy

This algorithm detects changes in echo amplitude caused by treated tissue, vapor bubbles, or cavitation bubbles induced by the HIFU energy delivery. It is normalized by the pre-lesion reference line to detect changes resulting only from the HIFU delivery to the current site.

$$p(n, T) = \frac{E_{signal} - E_{reference}}{E_{reference}} \quad (1)$$

$$E_{signal} = \sum_{window(n)} echo(n, T)^2 \quad E_{reference} = \sum_{window(n)} echo(n, T_0)^2 \quad (2,3)$$

Tissue Displacement

This algorithm detects changes in the displacement of the tissue due to the temperature-dependent speed of sound changes and the coefficient of thermal expansion of tissue due to the elevated tissue temperature induced by the HIFU energy delivery [4]. It is normalized by detecting differential displacements only with respect to the previous echo line.

$$p(n, T) = displacement[echo(n, T - \Delta T), echo(n, T)] \quad (4)$$

Signal Entropy

This algorithm detects changes in the shape of the overall RF backscattered data caused by treated tissue, vapor bubbles, or cavitation bubbles induced by the HIFU energy delivery. It is normalized by the pre-lesion reference line to detect changes resulting only from the HIFU delivery to the current site.

$$p(n, T) = H_{signal} - H_{reference} \quad (5)$$

$$H_{signal} = \sum_{k=0}^{N-1} p_{k(signal)} \cdot \log_2(p_{k(signal)}) \quad H_{reference} = \sum_{k=0}^{N-1} p_{k(reference)} \cdot \log_2(p_{k(reference)}) \quad (6,7)$$

In equations 6 and 7, p_k indicates the probability that the symbol k is present in the echo window signal, and $N = 2^b - 1$, where b is the number of quantization bits [10].

Attenuation Slope

This algorithm detects changes in the attenuation coefficient (slope) of the tissue due to the tissue temperature increases and the delivered HIFU dose [2,11]. It is normalized by the pre-lesion reference line to detect changes resulting only from the HIFU delivery to the current site:

$$p(n, T) = \text{slope at } f_c \text{ of best line fit to } \Delta S \quad (8)$$

$$\Delta S = S_{signal} - S_{reference} \quad (9)$$

$$S_{signal} = 20 \log_{10}[| \text{fft}(\text{echo}(n, T)) |] \quad S_{reference} = 20 \log_{10}[| \text{fft}(\text{echo}(n, T_0)) |] \quad (10,11)$$

where f_c is the center frequency of the imaging transducer.

Attenuation Intercept

This algorithm detects changes in the attenuation of the tissue due to the tissue temperature increases and the delivered HIFU dose [2,11]. It is normalized by the pre-lesion reference line to detect changes resulting only from the HIFU delivery to the current site:

$$p(n, T) = \text{intercept at } f_c \text{ of best line fit to } \Delta S \quad (12)$$

where f_c is the center frequency of the imaging transducer, and ΔS , S_{signal} , and $S_{reference}$ are as defined in equations 9, 10, and 11.

RESULTS

All algorithms were evaluated against the *in vivo* data. Thermometry data collected during the *in vivo* experiments recorded temperatures above 85°C at the exposure sites, indicating that thermal lesions were created with the selected treatment parameters (3s HIFU "ON", 6s HIFU "OFF" for each site, at 30-37W Total Acoustic Power typical). Histology and gross pathology examination of the treated prostates confirmed the creation of thermal lesions. It was not possible to determine from the histological samples if every HIFU shot created a lesion, since over time elementary lesions merged into a large contiguous lesion due to heat conduction.

It was found (assuming a lesion was created for every HIFU exposure) that signal energy-based algorithms consistently outperformed all other algorithms investigated.

When properly calibrated, these algorithms track the lesion formation from the onset of the HIFU delivery and update the color screen overlay every 500 ms for real-time lesion formation visualization. Figure 3 shows the result of the signal energy-based detection algorithm overlaid on the B-mode image of the current treatment site (acquired as part of the HIFU treatment procedure at $T=5s$ after each HIFU shot delivery for conventional *visual* treatment feedback) for a sequence of 6 multiple lesions created linearly one after the next in a dog prostate.

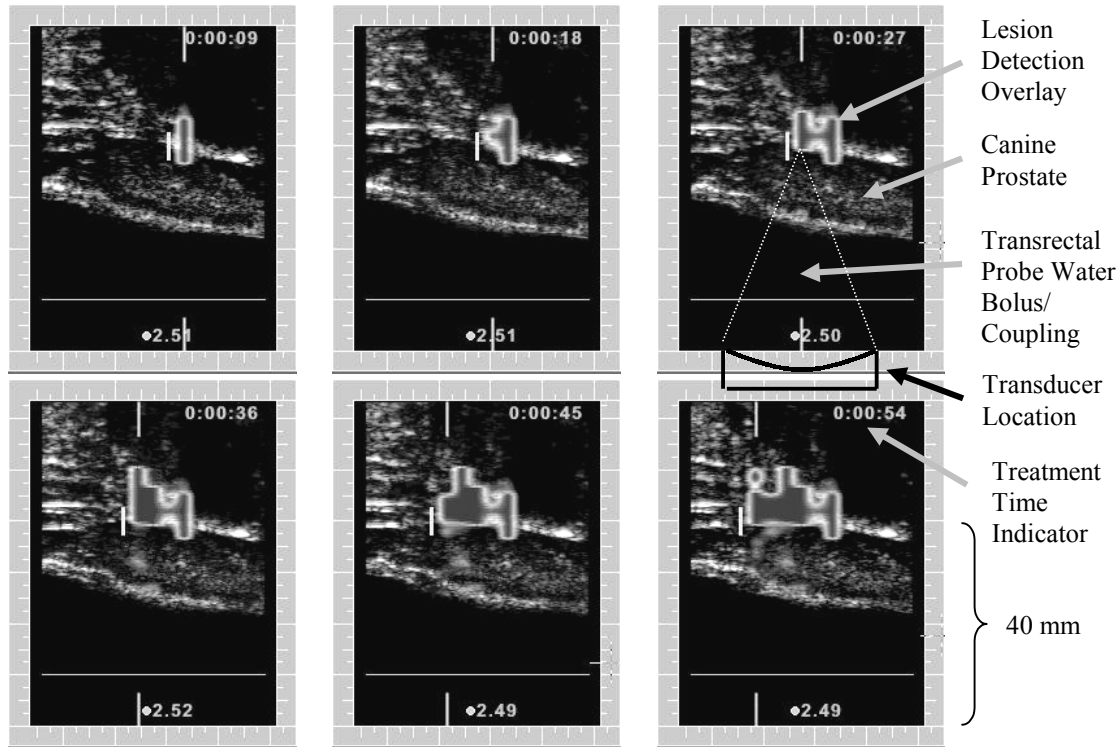


FIGURE 3. Real-time output of signal energy detection algorithm overlaid on the B-mode images of the current treatment site during a HIFU treatment of a dog prostate. 6 consecutive lesions are created with a 40 mm focal length HIFU transducer, from the prostate mid-section (top left image) to the bladder neck region (bottom right image).

DISCUSSION AND CONCLUSIONS

The results presented in this paper show that it is possible to implement a real-time detection algorithm that produces clinically useful results for HIFU treatment monitoring. Overlaying treatment feedback data on the conventional B-mode ultrasound images is an effective and intuitive way to present such information to the user. Accurate and consistent acquiring, computing, and displaying this information is the first step for implementing automated HIFU treatment control.

The results presented in this paper also show that developing and verifying algorithms to detect and image multiple lesions (such as those needed to ablate large tissue volumes via their superposition) give rise to additional problems and challenges not encountered in single-lesion imaging: (i) tissue properties change from one HIFU

shot to the next, (ii) individual lesions can merge to form a contiguous lesion, and (iii) ambiguities are created when one lesion is placed in a site already containing a lesion.

In order to address (i) and (ii) above, all of the developed algorithms have focused on measuring a relative change in tissue properties, using pre-HIFU reference lines (acquired pre-treatment at $T=-\infty$ and pre-lesion at $T=0s$) for parameter normalization and calibration. It was found that for *in vivo* implementations, the pre-treatment reference echo line is not well suited for calibration purposes of the detection algorithm: it de-correlates with respect to the pre-lesion echo within several minutes into the treatment due to HIFU-induced tissue changes and small probe/patient motion. The pre-lesion reference echo line, on the other hand, is extremely useful (and possibly even required) for the normalization of the detection algorithm. Using it as a reference ensures that only tissue changes induced by the current HIFU shot are detected.

Currently, out of all detection algorithms examined, the simple signal energy based detection algorithm has proven to be the most effective algorithm for non-invasively detecting (directly or indirectly) HIFU-induced lesions.

Even though these results are encouraging, it is believed that none of the algorithms developed thus far directly image the complete production of the lesion, but detect indirect indications that a lesion has been created, such as the presence of cavitation or vapor bubbles, or temperature rises. For any algorithm to be considered a direct (single or multiple) lesion imaging algorithm, we believe that it must meet the following criteria:

1. It must be able to localize the lesion in the tissue.
2. It must be able to follow the lesion creation process (i.e. be able to accurately track lesion size changes during HIFU delivery).
3. Its lesion size and shape estimates must agree with histo-pathological lesion size and shape estimates to a given tolerance.

For any algorithm to be considered a direct multiple lesion imaging algorithm, we believe that it must meet all of the criteria defined above, and:

4. Its lesion estimation methodology must be independent of the treatment time-history.

The signal energy-based multiple lesion detection algorithm is effective for point 1, relatively effective for point 2, but not very effective for point 3 (see irregular estimates of lesion shapes in Figure 3). Normalization has allowed the algorithm to be somewhat effective for point 4, but current clinical results still show a reduction in the magnitude of the parameter $p(n, T)$ as a function of treatment time T . For these reasons, the signal energy algorithm (as well as the others examined so far) currently fall into the category of indirect multiple lesion detection algorithms.

It is believed that the signal energy lesion detection algorithm is (at least partially) sensitive to cavitation and/or vapor bubbles. These are indirect lesion indicators, since their presence would indicate high intensities and temperatures that also create HIFU lesions, but do not necessarily outline the thermal lesion itself. Experiments are currently planned to test this hypothesis by suppressing cavitation and vapor bubble formation during HIFU using overpressure.

The pre-focal zone of the *in vivo* data was also analyzed to try to image purely thermal tissue changes not subject to possible cavitation or vapor bubbles, but still

subject to elevated temperatures as indirect indicators of thermal HIFU lesions. The results of this analysis are as of yet inconclusive. It is believed, however, that a pre-focal data analysis can provide useful lesion information, and work continues in this area.

Finally, the results also indicate that both direct and indirect lesion detection or lesion imaging methods can be clinically useful tools for the evaluation and control of HIFU treatments. Work continues on algorithm development, data acquisition methodologies, calibration, and implementation into the Sonablate[®] device for clinical applications in human prostate cancer treatments using HIFU.

ACKNOWLEDGMENTS

We would like to thank Dr. T.A. Gardner, MD., Dr. M.O. Koch, MD., and the staff of The Indiana University School Of Medicine at LARC for their help with the *in vivo* canine experiments. This work was partially funded by NIH SBIR Grant: 2 R44 CA83244-02.

REFERENCES

1. Wear, K., Wagner, R., Insana, M., Hall, T., "Application of Autoregressive Spectral Analysis to Cepstral Estimation of Mean Scatterer Spacing" in *IEEE Transactions on Ultrasonics, Ferroelectrics, and Frequency Control*, Vol. 40, pp. 50-58, 1993.
2. Greenleaf, J.F., *Tissue Characterization with Ultrasound*, Boca Raton: CRC Press, 1986.
3. Ribault, M., Chapelon, J.Y., Cathignol, D., and Gelet, A., "Differential Attenuation Imaging for the Characterization of High Intensity Focused Ultrasound Lesions" in *Ultrasound Imaging*, Vol. 20, pp. 160-177, 1998.
4. Seip, R., Feedback for Ultrasound Thermotherapy, Ph.D. Dissertation, The University of Michigan, 1996.
5. Fry, F.J., Sanghvi, N.T., Morris, R.F., Smithson, S., Atkinson, L., Dines, K., Franklin, T., and Hastings, J., "A Focused Ultrasound System for Tissue Volume Ablation in Deep Seated Brain Sites" in *Ultrasonics Symposium Proceedings*, Vol. 1, 1001-1004, 1986.
6. Bevan, P.D., and Sherar, M.D., "B-Scan Ultrasound Imaging of Thermal Coagulation in Bovine Liver: Frequency Shift Attenuation Mapping" in *Ultrasound in Medicine and Biology*, Vol. 27, No. 6, pp. 809-817, 2001.
7. Muschter, R., Bohlen, D., Thuroff, S., Ebert, T., and Madersbacher, S., "High Intensity Focused Ultrasound in Urology: Consensus Report", *High Energy Shock Waves in Medicine: Clinical Application in Urology, Gastroenterology, and Orthopedics*, Georg Thieme Verlag, Stuttgart - New York, 1997, pp. 140-146.
8. Sanghvi, N.T., Fry, F.J., Bihrl, R., Foster, R.S., Phillips, M.H., Syrus, J., Zaitsev, A.V., and Hennige, C.W., "Non-Invasive Surgery of Prostate Tissue by High Intensity Focused Ultrasound" in *IEEE Transactions on Ultrasonics, Ferroelectrics, and Frequency Control*, Vol. 43, pp. 1099-1110, 1996.
9. Madersbacher, S. and Marberger, M., "High-Intensity Focused Ultrasound in Urology," *J. of Endourology*, Vol. 9, No. 1, pp. 5-15, 1996.
10. Hughes, M.S., "Analysis of Ultrasonic Waveforms using Shannon Entropy," in *Ultrasonics Symposium Proceedings*, Vol. 2, 1205- 1208, 1992.
11. Damianou, C.A., Sanghvi, N.T., Fry, F.J., and Maass-Moreno, R., "Ultrasonic Attenuation and Absorption Dependence on Temperature and Thermal Dose in Dog Soft Tissue," in *J. Acoust. Soc. Am.*, July 1997.